

Towards Exploratory Landscape Analysis for Large-scale Optimization: A Dimensionality Reduction Framework

Ryoji Tanabe

Yokohama National University & Riken AIP
Yokohama, Kanagawa, Japan
rt.ryoji.tanabe@gmail.com

ABSTRACT

Although exploratory landscape analysis (ELA) has shown its effectiveness in various applications, most previous studies focused only on low- and moderate-dimensional problems. Thus, little is known about the scalability of the ELA approach for large-scale optimization. In this context, first, this paper analyzes the computational cost of features in the `flacco` package. Our results reveal that two important feature classes (`ela_level` and `ela_meta`) cannot be applied to large-scale optimization due to their high computational cost. To improve the scalability of the ELA approach, this paper proposes a dimensionality reduction framework that computes features in a reduced lower-dimensional space than the original solution space. We demonstrate that the proposed framework can drastically reduce the computation time of `ela_level` and `ela_meta` for large dimensions. In addition, the proposed framework can make the cell-mapping feature classes scalable for large-scale optimization. Our results also show that features computed by the proposed framework are beneficial for predicting the high-level properties of the 24 large-scale BBOB functions.

CCS CONCEPTS

• **Mathematics of computing** → **Evolutionary algorithms.**

KEYWORDS

Exploratory landscape analysis, fitness landscape analysis, large-scale black-box optimization, dimensionality reduction

ACM Reference Format:

Ryoji Tanabe. 2021. Towards Exploratory Landscape Analysis for Large-scale Optimization: A Dimensionality Reduction Framework. In *2021 Genetic and Evolutionary Computation Conference (GECCO '21), July 10–14, 2021, Lille, France*. ACM, New York, NY, USA, 10 pages. <https://doi.org/10.1145/3449639.3459300>

1 INTRODUCTION

General context. We consider a *noiseless* black-box optimization of an objective function $f : \mathbb{X} \rightarrow \mathbb{R}$, where $\mathbb{X} \subseteq \mathbb{R}^n$ is the n -dimensional solution space. This problem involves finding a solution $\mathbf{x} \in \mathbb{X}$ with an objective value $f(\mathbf{x})$ as small as possible without any explicit knowledge of f . Fitness landscape analysis [24, 36] is generally used to understand the high-level properties of a problem.

GECCO '21, July 10–14, 2021, Lille, France

© 2021 Association for Computing Machinery.

This is the author's version of the work. It is posted here for your personal use. Not for redistribution. The definitive Version of Record was published in *2021 Genetic and Evolutionary Computation Conference (GECCO '21), July 10–14, 2021, Lille, France*, <https://doi.org/10.1145/3449639.3459300>.

Table 1: Dimension n of the BBOB functions in selected previous studies for the following four tasks: high-level property classification (HP), algorithm selection (AS), performance prediction (PP), and per-instance algorithm configuration (PIAC).

Ref.	Year	Task	Dimension n
[25]	2011	HP	$n \in \{5, 10, 20\}$
[32]	2012	PP	$n \in \{2, 3, 5, 10, 20\}$
[5]	2012	AS	$n \in \{5, 10, 20\}$
[16]	2014	HP	$n = 2$
[17]	2015	HP	$n \in \{2, 3, 5, 10\}$
[33]	2015	HP	$n \in \{2, 5, 10, 20\}$
[18]	2016	HP	$n \in \{2, 3, 5, 10\}$
[2]	2016	PIAC	$n \in \{2, 3, 5, 10\}$ train: $n \in \{2, 4, 5, 8, 10, 16, 20, 32, 40, 64\}$ test: $n \in \{2, 4, 8, 10, 16, 20, 32, 40, 50, 66, 100\}$
[4]	2017	PIAC	$n \in \{2, 3, 5\}$
[7]	2019	HP, AS	$n \in \{2, 3, 5\}$
[19]	2019	AS	$n \in \{2, 3, 5, 10\}$
[13]	2020	PP	$n = 5$
[39]	2020	HP	$n = 5$
[8]	2020	HP	$n = 5$

Exploratory landscape analysis (ELA) [25, 26] provides a set of numerical low-level features based on a small sample of solutions. Unlike traditional analysis methods (e.g., FDC [15] and evolvability [43]), most ELA feature values are not human-interpretable [20]. In the ELA approach, the extracted features are used to characterize a fitness landscape of a black-box optimization problem by machine learning. As shown in Table 1, the ELA approach has been successfully applied to various tasks.

Table 1 shows the dimension n of the BBOB functions [11] in each previous study. This paper denotes *the noiseless BBOB functions* as *the BBOB functions*. As seen from Table 1, most previous studies¹ focused only on low- and moderate-dimensional problems, typically with $n \leq 20$. Thus, the scalability of the ELA approach for large-scale optimization has been poorly understood. This limits the applicability of the ELA approach. Although large-scale real-world problems can be found in a wide range of research areas (e.g., [9, 31]), a rule of thumb is not available. Note that this situation is not unique to ELA. Except for [29], most previous studies of fitness landscape analysis for black-box numerical optimization (e.g., [28, 30, 41]) focused only on relatively low-dimensional problems.

Contributions. In this context, first, we investigate the computation time of features in the R-package `flacco` [20], which currently provides 17 feature classes. We use the BBOB function set and its large-scale version [48], which consists of the 24 functions with $n \in \{20, 40, 80, 160, 320, 640\}$. The computation time of the ELA

¹A clear exception is [4]. For the sake of validation, n was different in the training and testing phases. The BBOB functions were used only for the training phase. The test functions with $n = 100$ were used to validate a performance prediction model, rather than to investigate the scalability of the ELA approach. The results in [4] showed that the performance prediction model does not work well when n in the testing phase is much larger than n in the training phase (i.e., $n = 100$).

features has been paid little attention in the literature. While some previous studies (e.g., [5, 7, 18]) used the terms “computationally cheap/expensive” to represent a necessary sample size for ELA, this paper uses the terms only to represent the wall-clock time for computing features. In [20], the computation time of the 17 feature classes in `flacco` was investigated on a problem with $n = 2$. In contrast, we analyze the influence of n on the computation time of some feature classes. The `ela_level` and `ela_meta` feature classes are one of the original six ELA feature classes [25]. Some previous studies (e.g., [13, 17–19, 25]) also reported their importance for various tasks. However, we demonstrate that the `ela_level` and `ela_meta` features are not available for $n \geq 320$ due to their high computational cost. Apart from the computational cost, as pointed out in [20], the four cell mapping feature classes (`cm_angle`, `cm_conv`, `cm_grad`, and `gcm`) [16] can be applied only to small-scale problems due to their properties. Thus, not all the 17 feature classes in `flacco` are available for large-scale optimization.

To improve the scalability of the ELA approach, we propose a dimensionality reduction framework that computes features in a reduced m -dimensional space instead of the original n -dimensional solution space, where $m < n$ (e.g., $m = 2$ and $n = 640$). The proposed framework is inspired by dimensionality reduction strategies in Bayesian optimization [12, 38, 45, 51]. In this paper, we use the weighting strategy-based principal component analysis (PCA) procedure in PCA-assisted Bayesian optimization (PCA-BO) [38] for dimensionality reduction. Since the proposed framework computes features in a reduced lower-dimensional space \mathbb{R}^m than the original solution space $\mathbb{X} \subseteq \mathbb{R}^n$, it can drastically reduce the computation time. In addition to the computational cost reduction, the proposed framework can make the cell mapping feature classes scalable for large-scale optimization. We evaluate the effectiveness of the proposed framework for predicting the high-level properties of the 24 BBOB functions with up to 640 dimensions.

Related work. The proposed framework is the first attempt to compute features in a reduced m -dimensional space in the field of black-box numerical optimization. We emphasize that dimensionality reduction is performed in *the solution space, not the feature space*. While some previous studies (e.g., [8, 34, 41, 50]) applied PCA [42] to the feature space for the sake of visualization, we apply PCA to the solution space. In the field of combinatorial optimization, some previous studies (e.g., [44, 49]) applied dimensionality reduction methods to the solution space for the sake of visualization. In contrast, we are not interested in such a visualization.

Belkhir et al. proposed a surrogate-assisted framework that computes features based on a small-sized sample \mathcal{X} [3]. In their framework, an augmented solution $\mathbf{x}^{\text{aug}} \notin \mathcal{X}$ is evaluated by a surrogate model $M : \mathbb{R}^n \rightarrow \mathbb{R}$ instead of the actual objective function f . Then, \mathbf{x}^{aug} is added to an augmented sample \mathcal{X}^{aug} . Finally, features are computed based on the union of \mathcal{X} and \mathcal{X}^{aug} . Their framework and our framework are similar in that the features are not computed based only on the original sample \mathcal{X} . However, their framework does not aim to reduce the dimension of the solution space.

We are interested in a speed-up technique at the algorithm level, not the implementation level. One may think that the scalability issue can be addressed by reimplementing `flacco` in any compiled language (e.g., C). However, it is not realistic to reimplement `flacco`

without useful R libraries (e.g., `mlr`). Reimplementing `flacco` is also not a fundamental solution for the scalability issue.

Outline. Section 2 provides some preliminaries. Section 3 investigates the computation time of ELA features. Section 4 explains the proposed framework. Section 5 explains our experimental setting. Section 6 shows our analysis results. Section 7 concludes this paper.

Code availability. The source code of the proposed framework is available at https://github.com/ryojitanabe/ela_drframework.

Supplementary file. Throughout this paper, we refer to a figure and a table in the supplementary file (<https://ryojitanabe.github.io/pdf/gecco21-supp.pdf>) as Figure S.* and Table S.*, respectively.

2 PRELIMINARIES

Section 2.1 explains the BBOB functions and their high-level properties. Section 2.2 describes ELA. Section 2.3 explains PCA-BO [38].

2.1 BBOB function set

The BBOB function set [11] consists of the 24 functions to evaluate the performance of optimizers in terms of difficulties in real-world black-box optimization. The functions f_1, \dots, f_{24} are grouped into the following five categories: separable functions (f_1, \dots, f_5), functions with low or moderate conditioning (f_6, \dots, f_9), functions with high conditioning and unimodal (f_{10}, \dots, f_{14}), multimodal functions with adequate global structure (f_{15}, \dots, f_{19}), and multimodal functions with weak global structure (f_{20}, \dots, f_{24}). Each BBOB function further consists many instances. The large-scale version of the BBOB function set [48] provides problems with up to $n = 640$.

Table 2 shows the following seven high-level properties of the 24 BBOB functions [25]: multimodality, global structure, separability, variable scaling, search space homogeneity, basin sizes, and global to local optima contrast. For each BBOB function, the degree of a high-level property was categorized by experts, e.g., “none”, “low”, “medium”, and “high” for multimodality. Since some high-level properties presented in [25] were inappropriately classified, we slightly revised them in this work. As in [17], we classified the global structure property of the 13 unimodal functions as “strong”. Since the Lunacek bi-Rastrigin function f_{24} [23] clearly has a multi-funnel structure, we classified its global structure property as “deceptive”. As in [27], we revised the separability property of f_3 , f_6 , and f_7 . According to the definitions in [11], we revised the variable scaling and global to local optima contrast properties of some functions.

2.2 ELA

ELA [25] produces a set of numerical features based on a set of l solutions $\mathcal{X} = \{\mathbf{x}_i\}_{i=1}^l$, where \mathcal{X} is called the initial sample. In general, \mathcal{X} is randomly generated in the n -dimensional solution space $\mathbb{X} \subseteq \mathbb{R}^n$ by a sampling method (e.g., Latin hypercube sampling). Then, the objective value $f(\mathbf{x})$ is calculated for each solution $\mathbf{x} \in \mathcal{X}$. Let \mathcal{Y} be $\{f(\mathbf{x}_i)\}_{i=1}^l$. We also denote a pair of \mathcal{X} and \mathcal{Y} as a data set \mathcal{D} . Finally, an ELA feature maps \mathcal{D} to a numerical value.

The R-package `flacco` [20] is generally used to compute features. Currently, `flacco` provides 17 feature classes. Each feature class consists of more than one feature. For example, the `ela_distr` class provides the five features: `skewness`, `kurtosis`, `number_of_peaks`, `costs_fun_evals`, and `costs_runtime`.

Table 2: High-level properties of the 24 BBOB functions. The properties revised from [26] are highlighted.

	multim.	gl-struct.	separ.	scaling	homog.	basin	gl-cont.
f_1	none	strong	high	none	high	none	none
f_2	none	strong	high	high	high	none	none
f_3	high	strong	high	low	high	low	low
f_4	high	string	high	low	high	med.	low
f_5	none	strong	high	low	high	none	none
f_6	none	strong	none	low	med.	none	none
f_7	none	strong	none	low	high	none	none
f_8	low	strong	none	low	med.	low	low
f_9	low	strong	none	low	med.	low	low
f_{10}	none	strong	none	high	high	none	none
f_{11}	none	strong	none	high	high	none	none
f_{12}	none	strong	none	high	high	none	none
f_{13}	none	strong	none	med.	med.	none	none
f_{14}	none	strong	none	med.	med.	none	none
f_{15}	high	strong	none	low	high	low	low
f_{16}	high	med.	none	med.	high	med.	low
f_{17}	high	med.	none	low	med.	med.	high
f_{18}	high	med.	none	high	med.	med.	high
f_{19}	high	strong	none	low	high	low	low
f_{20}	med.	dec.	none	low	high	low	high
f_{21}	med.	none	none	med.	high	med.	low
f_{22}	low	none	none	high	high	med.	high
f_{23}	high	none	none	low	high	low	low
f_{24}	high	dec.	none	low	high	low	low

Table 3 shows 14 feature classes provided by flacco. The original six ELA feature classes [25] are `ela_conv`, `ela_curv`, `ela_local`, `ela_distr`, `ela_level`, and `ela_meta`. As in most recent studies (see Table 1), we do not consider `ela_conv`, `ela_curv`, and `ela_local`. This is because they require additional function evaluations independently from the initial sample \mathcal{X} .

The `ela_distr` features are with regard to the distribution of \mathcal{Y} . The `ela_level` class splits \mathcal{D} into binary classes based on a pre-defined threshold value. Then, three classifiers (LDA, QDA, and MDA) are used to classify an objective value $f(x) \in \mathcal{Y}$. Each `ela_level` feature represents the mean misclassification errors of a classifier over a 10-fold cross-validation. The `ela_meta` class fits linear and quadratic regression models to \mathcal{D} . The `ela_meta` features are the model-fitting results, e.g., the adjusted R^2 .

The `nb` features aim to detect funnel structures by using the nearest-better clustering method [37], which was originally proposed for multimodal optimization. The `disp` class is an extension of the dispersion metric [22], which is one of the most representative metrics for landscape analysis. The `ic` class provides features regarding the information content of fitness sequences [33].

As the name suggests, the `basic` features provide basic information about \mathcal{D} , e.g., the size of \mathcal{X} and the maximum value of \mathcal{Y} . The `limo` class fits a linear model to \mathcal{X} as the explanatory variables and \mathcal{Y} as the dependent variables. The `pca` class applies PCA to \mathcal{X} and \mathcal{D} separately. The `pca` features are based on the covariance and the correlation matrix calculated by PCA [42].

The cell mapping feature classes (`cm_angle`, `cm_grad`, `cm_conv`, `gcm`, and `bt`) [16, 20] discretize the n -dimensional solution space into b^n cells, where b is the number of blocks for each dimension. The minimum value of b is 3 [20]. Note that the number of cells b^n

Table 3: 14 feature classes provided by flacco, except for `ela_conv`, `ela_curv`, and `ela_local`.

Feature class	Name	Num. features
<code>ela_distr</code> [25]	<i>y</i> -distribution	5
<code>ela_level</code> [25]	levelset	20
<code>ela_meta</code> [25]	meta-model	11
<code>nb</code> [17]	nearest better clustering (NBC)	7
<code>disp</code> [17]	dispersion	18
<code>ic</code> [33]	information content	7
<code>basic</code> [20]	basic	15
<code>limo</code> [20]	linear model	14
<code>pca</code> [20]	principal component analysis	10
<code>cm_angle</code> [16]	cell mapping angle	10
<code>cm_conv</code> [16]	cell mapping convexity	6
<code>cm_grad</code> [16]	cell mapping gradient homog.	6
<code>gcm</code> [16]	generalized cell mapping	75
<code>bt</code> [20]	barrier tree	90

grows exponentially with respect to n . For example, $b^n \approx 3.5 \times 10^9$ for $b = 3$ and $n = 20$. For this reason, the cell mapping feature classes can be applied only to low-dimensional problems [20]. The `cm_angle` and `cm_grad` features are mainly based on the angle and gradient of the position of solutions in a cell, respectively. The `cm_conv` class aims to characterize the convexity of the fitness landscape. Most `gcm` features are based on the transition probability to move from a cell to one of its neighbors. The `bt` features aim to capture the local optimal solutions and the ridges of the fitness landscape based on the leaves of the tree and the branching nodes.

2.3 PCA-BO

Bayesian optimization is an efficient sequential model-based approach for computationally expensive optimization [40]. The Gaussian process regression (GPR) model is generally used in Bayesian optimization. However, it is difficult to apply the GPR model to large-scale problems. This is because the GPR model requires high computational cost as the dimension increases. One promising way to address this issue is the use of dimensionality reduction [12, 38, 45, 51]. A similar approach has been adopted in the field of evolutionary computation (e.g., [21]).

PCA-assisted Bayesian optimization (PCA-BO) [38] uses PCA to reduce the original dimension n to a lower dimension m ($m < n$). PCA-BO also uses a weighting strategy to incorporate the information about the objective values into solutions so that a better solution is treated as more important than other solutions.

At the beginning of each iteration, PCA-BO re-scales a set of l solutions found so far $\mathcal{X} = \{\mathbf{x}\}_{i=1}^l$ by the weighting strategy. First, all the solutions in \mathcal{X} are ranked based on their objective values. For $i \in \{1, \dots, l\}$, a weight value w_i is assigned to the i -th solution $\mathbf{x}_i \in \mathcal{X}$ based on its rank r_i as follows: $w_i = \tilde{w}_i / \sum_{j=1}^l \tilde{w}_j$, where $\tilde{w}_i = \ln l - \ln r_i$. Then, \mathbf{x}_i is re-scaled as follows: $\tilde{\mathbf{x}}_i = w_i(\mathbf{x}_i - \mathbf{m})$, where $\mathbf{m} = 1/l \sum_{\mathbf{x} \in \mathcal{X}} \mathbf{x}$ is the mean vector of \mathcal{X} . After the re-scaled version $\tilde{\mathcal{X}}$ of \mathcal{X} is obtained by the weighting strategy, PCA-BO applies PCA to $\tilde{\mathcal{X}}$. The dimensionality of each point in $\tilde{\mathcal{X}}$ is reduced from n to m . In other words, PCA maps an n -dimensional point $\tilde{\mathbf{x}} \in \mathbb{R}^n$ to an m -dimensional point $\hat{\mathbf{x}} \in \mathbb{R}^m$. Then, PCA-BO fits a GPR model to $\hat{\mathcal{X}} = \{\hat{\mathbf{x}}\}_{i=1}^l$ and searches a candidate solution that maximizes the acquisition function in \mathbb{R}^m .

3 COMPUTATIONAL COST ISSUE IN ELA

Here, we investigate the computation time of the nine non-cell mapping ELA feature classes in Table 3 on problems with up to $n = 640$. Since the cell mapping features can be computed only for small dimensions, we do not consider them in this section.

Apart from the features, we point out that the improved Latin hypercube sampling method (IHS) [1] in `f1acco` is time-consuming for large dimensions. Our results show that IHS requires approximately 6.6 hours for sampling $50 \times n$ solutions on a problem instance for $n = 160$. The procedure of IHS did not finish within one day for $n \geq 320$. For details, see Figure S.1. This is because IHS calculates the Euclidean distance between points every time IHS adds a new point. For this reason, we use Latin hypercube sampling (LHS) instead of IHS throughout this paper.

3.1 Experimental setup

We conducted all experiments on a workstation with an Intel(R) 40-Core Xeon Gold 6230 (20-Core \times 2) 2.1GHz and 384GB RAM using Ubuntu 18.04. We used Python version 3.8 and R version 3.6.3. We used the Python interface of `f1acco` (`pf1acco`), which is available at <https://github.com/Reiyan/pf1acco>. We believe that the time to call a `f1acco` function from `pf1acco` is negligible when n is large enough. We used the BBOB function set [11] for $n \in \{2, 3, 5, 10\}$ and its large-scale version [48] for $n \in \{20, 40, 80, 160, 320, 640\}$. Both function sets are available in the COCO platform [10]. We performed 31 independent runs on the first instance of f_1 to measure the average time for computing features. We used `lhs` in the `pyDOE` package to generate the initial sample \mathcal{X} . As recommended in [18], we set $|\mathcal{X}|$ to $50 \times n$ (i.e., $l = 50 \times n$ in Section 2.3). We did not take into account the time to generate \mathcal{X} and evaluate their objective values \mathcal{Y} . Thus, we measured only the time to compute features.

3.2 Feature computation time in ELA

Figure 1 shows the average computation time of each feature class over 31 runs. We explain results of `d_ela_level` and `d_ela_meta` in Section 6.1. It seems that the computation time of all the feature classes (except for `ela_distr`) increases exponentially with respect to n . Note that the computation time is influenced by both n and $|\mathcal{X}|$. Figure S.2 shows results when fixing $|\mathcal{X}|$ to 100. Figure S.3 shows results when fixing n to 2. Although setting $|\mathcal{X}|$ to a small constant number (i.e., $|\mathcal{X}| = 100$) can speed up the computation of features, the resulting features are likely to be ineffective.

As seen from Figure 1, the computation time of `basic` is lowest for $n \leq 80$. For $n \geq 160$, `ela_distr` is the fastest feature class in terms of the computation time, where the number of the `ela_distr` features is only five (see Table 3). Since the `ela_distr` features are based only on the objective values \mathcal{Y} , its computational cost depends only on $|\mathcal{Y}|$. Since `limo` and `pca` are based on relatively simple linear models, their computational cost is acceptable even for $n = 640$. The single-run computation of the `limo` and `pca` features took approximately 3.5 minutes and 1.1 minutes for $n = 640$, respectively. For $n \geq 40$, `ic`, `nbc`, and `disp` perform relatively similar in terms of the computation time. This is because the three feature classes calculate the distance between solutions in \mathcal{X} , where the distance calculation time depends on n and $|\mathcal{X}|$.

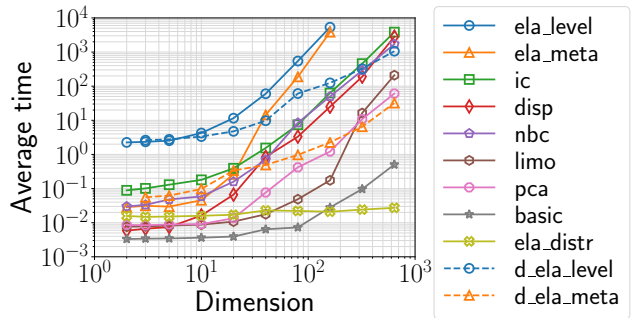


Figure 1: Average feature computation time (sec) on the first instance of f_1 with $n \in \{2, 3, 5, 10, 20, 40, 80, 160, 320, 640\}$.

The computational cost of the `ela_meta` features is relatively low for $n \leq 20$, but it increases drastically for $n \geq 40$. This is mainly because fitting a quadratic model in `ela_meta` is time-consuming for large dimensions. Clearly, the computation of `ela_level` features are based on results of the three classifiers in a 10-fold cross-validation as explained in Section 2.2. As shown in Figure 1, the single-run computation of the `ela_meta` and `ela_level` features took approximately 1.1 hours and 1.5 hours for $n = 160$, respectively. We could not measure the computation time of the `ela_level` and `ela_meta` features for $n \geq 320$ because their single-run computation for $n = 320$ did not finish within 3 days.

4 PROPOSED FRAMEWORK

Our results in Section 3 showed that the two important feature classes (`ela_level` and `ela_meta`) are not available for large-scale optimization due to their time-consuming process. Apart from that, as pointed out in [20], the cell mapping feature classes can be applied only to low-dimensional problems. To improve the scalability of these feature classes, we propose a simple dimensionality reduction framework. Let $\mathcal{X} = \{x_i\}_{i=1}^l$ be a set of l n -dimensional solutions, i.e., the initial sample. Let also $\mathcal{Y} = \{f(x_i)\}_{i=1}^l$ be a set of l objective values. As explained in Section 2.2, the features are computed based on \mathcal{X} and \mathcal{Y} . However, as discussed above, some features cannot be computed in a practical time when n is large.

One simple way of addressing this issue is to reduce the original dimension n to a lower dimension m as in dimensionality reduction strategies in Bayesian optimization. Previous studies (see Section 2.3) show that a dimensionality reduction strategy can effectively reduce the computational cost for fitting a surrogate model for large-scale optimization. Based on these promising results, we suppose that some (not all) features computed in the reduced m -dimensional space can substitute for their original versions.

In the proposed framework, first, a dimensionality reduction method is applied to \mathcal{X} . As a result, each solution $x \in \mathbb{R}^n$ in \mathcal{X} is mapped to a point $\hat{x} \in \mathbb{R}^m$, where $m < n$. Let $\hat{\mathcal{X}} = \{\hat{x}_i\}_{i=1}^l$ be a set of l m -dimensional points transformed from \mathcal{X} . For $i \in \{1, \dots, l\}$, the objective value $f(x_i)$ is assigned to \hat{x}_i without any change, i.e., $\hat{\mathcal{Y}} := \mathcal{Y}$. Thus, the proposed framework does not require additional

function evaluations. Finally, features are computed based on $\hat{\mathcal{X}}$ and $\hat{\mathcal{Y}}$ instead of \mathcal{X} and \mathcal{Y} .

Although any dimensionality reduction method can be integrated into the proposed framework, this paper uses the weighting strategy-based PCA approach in PCA-BO [38] (see Section 2.3). PCA is a simple linear transformation technique, but it is one of the most representative dimensionality reduction methods [47]. For this reason, PCA is a reasonable first choice. Note that the PCA procedure in PCA-BO is independent from the `pca` feature class.

One advantage of the proposed framework is that it can speed up the computation of time-consuming features since the features are computed in a reduced m -dimensional space. Another advantage is that the proposed framework can make the cell mapping feature classes scalable for large-scale optimization by setting m to a small value (e.g., $m = 2$). One disadvantage is that features computed by the proposed framework may be misleading. This is because it is impossible for the proposed framework to exactly extract all information about the original n -dimensional problem. For this reason, it is expected that the original features are more effective than their dimensionality reduction versions when they are available.

5 EXPERIMENTAL SETUP

This section explains the experimental setup. Unless explicitly noted, the computational environment is the same as in Section 3.1. As in most previous studies (e.g., [7, 16, 18, 25]), we used an off-the-shelf random forest classifier [6] for predicting the seven high-level properties of the 24 BBOB functions (see Table 2). We aim to examine the effectiveness of a feature set for the high-level property classification task rather than to achieve high accuracy by using a state-of-the-art classifier (e.g., deep neural network). We employed the scikit-learn implementation of random forest [35]. We set the number of trees to 1 000. According to the recommendation in [18], we set the size of the initial sample $|\mathcal{X}|$ ($= l$) to $50 \times n$.

Below, Section 5.1 explains feature sets investigated in Section 6. Section 5.2 describes the cross-validation procedure in this work.

5.1 Feature sets

Table 4 shows five feature sets investigated in this work. For a feature class computed by the proposed dimensionality reduction framework, we add a prefix “d_” to its original name. For dimensionality reduction, we employed the implementation of PCA-BO provided by the authors of [38] (<https://github.com/wangronin/Bayesian-Optimization>). We set the reduced dimension m to 2.

Our results in Section 3.2 show that the following seven feature classes are relatively computationally cheap for large dimensions: `ela_distr`, `basic`, `ic`, `disp`, `nbc`, `pca`, and `limo`. We denote a set of the seven computationally cheap feature classes as C7. We consider C7 as a base-line feature set for analysis. Morgan and Gallagher demonstrated that the performance of the dispersion metric [22] for large dimensions ($n \leq 200$) can be improved by normalization [29]. One may think that the `disp` features with normalization is more effective for large dimensions. However, our preliminary results showed that normalization does not strongly affect the `disp` features. This is mainly because the `disp` features are already normalized by the mean or the median of the dispersion value of the whole sample \mathcal{X} . Of course, further investigation is needed.

Table 4: Five feature sets investigated in this work.

Name	Feature classes
C7	{ <code>ela_distr</code> , <code>basic</code> , <code>ic</code> , <code>disp</code> , <code>nbc</code> , <code>pca</code> , <code>limo</code> }
C7-E2	$C7 \cup \{\text{ela_level}, \text{ela_meta}\}$
C7-D2	$C7 \cup \{\text{d_ela_level}, \text{d_ela_meta}\}$
C7-C4	$C7 \cup \{\text{gcm}, \text{cm_angle}, \text{cm_conv}, \text{cm_grad}\}$
C7-D4	$C7 \cup \{\text{d_gcm}, \text{d_cm_angle}, \text{d_cm_conv}, \text{d_cm_grad}\}$

C7-E2 is a C7 with the two computationally expensive feature classes (`ela_level` and `ela_meta`), which can be computed only for $n \leq 160$ due to their time-consuming process. C7-D2 is a C7 with the dimensionality reduction versions of the two expensive feature classes. We analyze the effectiveness of the proposed framework by comparing C7-D2 with C7 and C7-E2.

C7-C4 is a C7 with the four cell mapping feature classes, which are available only for $n \leq 5$. Since `bt` can be computed only for $n = 2$, we did not use `bt`. C7-D4 is a C7 with the dimensionality reduction versions of the four cell mapping feature classes. Before computing the cell mapping features, we normalized each point \hat{x} in $\hat{\mathcal{X}}$ into the range $[0, 1]^m$ using the minimum and maximum values in $\hat{\mathcal{X}}$ for each dimension.

For each n , we deleted a feature that takes the same value on all instances (e.g., `disp.costs_fun_evals` and `basic.dim`). As in [4, 7, 39], we did not perform feature selection because it deteriorated the performance of a classifier in our preliminary experiment. A similar observation was reported in [14]. This may be due to a *leave-one-problem-out cross-validation* (LOPO-CV) [7, 16] (see the next section), where the prediction model is validated on an unseen function. Although an analysis of cross-validation methods is beyond the scope of this paper, an in-depth investigation is needed.

5.2 Cross-validation procedure

The ultimate goal of high-level property classification is to predict a high-level property of an unseen real-world problem. Thus, we need to evaluate the unbiased performance of a classifier on unseen test problem instances. For this reason, we adopted LOPO-CV [7, 16]. In LOPO-CV, a 24-fold cross-validation is performed on the 24 BBOB functions with each dimension n . Let \mathcal{I}_i be a set of problem instances of a function f_i , where $i \in \{1, \dots, 24\}$. Since each BBOB function consists of 15 instances in the COCO platform, $|\mathcal{I}_i| = 15$ for any f_i . While we used only the first instance of f_1 to measure the wall-clock time in Section 3, we consider all the 15 instances of all the 24 BBOB functions in Sections 6.2 and 6.3. In the i -th fold, \mathcal{I}_i (15 instances) is used in the testing phase. Thus, $\mathcal{I}_1 \cup \dots \cup \mathcal{I}_{24} \setminus \mathcal{I}_i$ ($23 \times 15 = 345$ instances) are used in the training phase. Since the 24 BBOB functions have totally different properties from each other (see Table 2), problem instances used in the training and testing phases are also different in LOPO-CV. For this reason, high-level property classification in LOPO-CV is very challenging.

We also evaluated the performance of a classifier by using a *leave-one-instance-out cross-validation* (LOIO-CV) [7]. In LOIO-CV, a 15-fold cross-validation is performed on the 15 problem instances. In the i -th fold, the 24 i -th problem instances are used in the testing phase. Thus, the remaining $14 \times 24 = 336$ instances are used in the training phase. Since problem instances used in the training

and testing phases are very similar, LOIO-CV is much easier than LOPO-CV. In fact, our preliminary results showed that some classifiers could perfectly predict some high-level properties of the 24 BBOB functions in LOIO-CV (i.e., accuracy = 1). For this reason, we consider only the more challenging LOPO-CV in this paper.

6 RESULTS

First, Section 6.1 demonstrates that the proposed framework can reduce the computational cost of the two expensive feature classes (`ela_meta` and `ela_level`) for large dimensions. Then, Section 6.2 examines the effectiveness of the five feature sets in Table 4 for predicting the high-level properties of the 24 large-scale BBOB functions. Finally, Section 6.3 analyzes the similarity between the original features and their dimensionality reduction versions.

For the sake of simplicity, we refer to “a random forest classification model using a feature set \mathcal{F} ” as “ \mathcal{F} ”. For example, we denote “the accuracy of a random forest classifier using C7-D2” as “the accuracy of C7-D2”.

6.1 Computation time reduction

Figure 1 (see Section 3.2) shows the average time for computing the `d_ela_level` and `d_ela_meta` features. In Figure 1, the computation time includes the PCA-BO procedure for dimensionality reduction. Since the proposed framework cannot be applied to problems with $n \leq m$, we do not show results of the `d_ela_level` and `d_ela_meta` features for $n = 2$. Figure S.4 shows results of the dimensionality reduction versions of the four cell mapping feature classes in C7-D4. They perform relatively similar to `pca` and `d_ela_meta` for $n = 640$.

As shown in Figure 1, the computation time of `d_ela_level` is slightly higher than that of `ela_level` for $n \in \{3, 5\}$. This is because the dimensionality reduction procedure is more time-consuming than the feature computation procedure for small dimensions. In contrast, `d_ela_level` is much faster than `ela_level` in terms of the computation time as the dimension increases. For example, while the computation of `ela_level` requires approximately 1.5 hours for $n = 160$, that of `d_ela_level` requires only approximately 2.1 minutes. Notably, the computation of `d_ela_level` is cheaper than that of the three distance-based feature classes (`ic`, `disp`, and `nbcc`) for $n = 640$. Results of `d_ela_meta` is similar to the results of `d_ela_level` discussed above. The computation of `d_ela_meta` is much cheaper than that of `ela_meta` for $n \geq 40$. Interestingly, `d_ela_meta` is faster than `pca` for $n \geq 320$ in terms of the computation time. As seen from Figure 1, the computation of `d_ela_meta` is faster than that of `limo` for $n \geq 320$. This result indicates that fitting a quadratic model in a reduced m -dimensional space can be faster than fitting a linear model in the original n -dimensional space as n increases. In summary, our results show that the proposed framework can effectively reduce the computation time of `ela_meta` and `ela_level` for large dimensions.

6.2 Effectiveness of features computed by the proposed framework

6.2.1 Results of C7, C7-E2, and C7-D2. Tables 5(a)–(g) show the average accuracy of C7, C7-E2, and C7-D2 for the seven high-level properties, respectively. Table 5(h) also shows the overall average.

In Table 5, “Na” means that the corresponding feature set is not available for a given n due to its time-consuming process. The best and second best data are highlighted by **dark gray** and **gray**, respectively. When only two data are available, only the best data is highlighted by **dark gray**. Note that we built one random forest model for each fold, each feature set, each classification task, and each dimension. Tables S.1 (a)–(g) also show the standard deviation of the accuracy. Due to LOPO-CV, the standard deviation is large.

As shown in Table 5, C7-E2 performs the best in terms of the accuracy in most cases for $n \leq 160$, except for the prediction of the homogeneity property. These results indicate the importance of the `ela_meta` and `ela_level` features to predict a high-level property of an unseen problem. However, C7-E2 is not available for ≥ 320 due to the high-computational cost of `ela_meta` and `ela_level`. In contrast, C7-D2 achieves better accuracy than C7 in most cases (especially for $n \geq 320$), except for the prediction of the separability property. These results indicate that the `d_ela_meta` and `d_ela_level` features can be substituted for their original versions for large-scale optimization. The `d_ela_meta` and `d_ela_level` features are particularly beneficial for predicting the multimodality and basin size properties (see Tables 5(a) and (f)). Since the proposed framework reduces the dimensionality of each point in the initial sample \mathcal{X} from n to m , it is unsurprising that the `d_ela_meta` and `d_ela_level` features do not provide meaningful information about separability. Consequently, for the prediction of the separability property, C7-D2 performs worse than C7 in terms of accuracy due to the misleading features (see Table 5(c)). As already discussed in Section 4, this is one disadvantage of the proposed framework.

The influence of the dimension n on the performance of the ELA approach has not been well analyzed in the literature. Intuitively, it is expected that a prediction model performs poorly as the dimension n increases. Roughly speaking, the results in Tables 5(a), (b), (c), and (d) are consistent with our intuition. In contrast, the results in Tables 5(e), (f), and (g) show that the accuracy of C7, C7-E2, and C7-D2 is improved as n increases. For example, the accuracy of C7 for predicting the homogeneity property is 0.633 and 0.772 for $n = 2$ and $n = 640$, respectively. This may be because the size of the initial sample \mathcal{X} increases linearly with respect to n , where we set $|\mathcal{X}|$ to $50 \times n$. The large-sized \mathcal{X} can possibly be beneficial to capture the degree of the three properties (homogeneity, basin size, and global to local optima contrast) independently from n .

6.2.2 Results of C7, C7-C4, and C7-D4. Table 6 shows the overall average accuracy of C7, C7-C4, and C7-D4. Table S.2 shows detailed results. As seen from Table 6, C7-C4 performs the best in terms of accuracy for $n \leq 5$. Although the cell mapping features are available only for $n \leq 5$, the proposed framework can improve their scalability for $n > 5$. As shown in the results of C7-D4, the cell mapping features computed by the proposed framework are helpful for high-level property classification for $n \geq 10$. However, C7-D4 performs poorly for small dimensions similar to C7-D2. Thus, it is better to use the proposed framework only for large dimensions.

6.2.3 Feature importance. We investigate which features are particularly important in C7-D2 and C7-D4. Table 7 shows the average rankings of the features computed by the proposed framework for $n = 640$. Results for all dimensions are relatively similar. First, we

Table 5: Average accuracy of C7, C7-E2, and C7-D2 on the 24 BBOB functions with $n \in \{2, 3, 5, 10, 20, 40, 80, 160, 320, 640\}$.

(a) Multimodality				(b) Global structure				(c) Separability				(d) Variable scaling			
	C7	C7-E2	C7-D2		C7	C7-E2	C7-D2		C7	C7-E2	C7-D2		C7	C7-E2	C7-D2
2	0.642	0.703	Na	2	0.758	0.786	Na	2	0.756	0.803	Na	2	0.581	0.586	Na
3	0.569	0.597	0.578	3	0.792	0.797	0.778	3	0.789	0.856	0.786	3	0.611	0.583	0.611
5	0.536	0.625	0.622	5	0.769	0.772	0.761	5	0.758	0.864	0.761	5	0.628	0.600	0.594
10	0.522	0.631	0.647	10	0.708	0.750	0.692	10	0.758	0.828	0.753	10	0.508	0.556	0.572
20	0.531	0.725	0.639	20	0.714	0.742	0.697	20	0.708	0.808	0.744	20	0.539	0.578	0.583
40	0.556	0.689	0.617	40	0.711	0.711	0.711	40	0.767	0.836	0.758	40	0.539	0.581	0.556
80	0.600	0.783	0.622	80	0.697	0.697	0.697	80	0.703	0.775	0.686	80	0.542	0.583	0.581
160	0.522	0.650	0.561	160	0.647	0.650	0.631	160	0.697	0.753	0.667	160	0.558	0.583	0.583
320	0.544	Na	0.578	320	0.664	Na	0.667	320	0.722	Na	0.669	320	0.547	Na	0.583
640	0.514	Na	0.583	640	0.667	Na	0.678	640	0.725	Na	0.669	640	0.542	Na	0.542

(e) Homogeneity				(f) Basin size				(g) Global to local optima cont.				(h) Overall average			
	C7	C7-E2	C7-D2		C7	C7-E2	C7-D2		C7	C7-E2	C7-D2		C7	C7-E2	C7-D2
2	0.633	0.636	Na	2	0.450	0.492	Na	2	0.572	0.642	Na	2	0.627	0.664	Na
3	0.664	0.608	0.608	3	0.544	0.547	0.522	3	0.586	0.600	0.572	3	0.651	0.656	0.637
5	0.647	0.578	0.647	5	0.508	0.628	0.522	5	0.497	0.669	0.536	5	0.621	0.677	0.635
10	0.722	0.658	0.769	10	0.494	0.608	0.636	10	0.542	0.656	0.619	10	0.608	0.669	0.670
20	0.772	0.731	0.731	20	0.467	0.647	0.558	20	0.544	0.728	0.617	20	0.611	0.708	0.653
40	0.761	0.700	0.744	40	0.531	0.617	0.614	40	0.533	0.708	0.597	40	0.628	0.692	0.657
80	0.703	0.639	0.742	80	0.464	0.650	0.597	80	0.558	0.703	0.619	80	0.610	0.690	0.649
160	0.656	0.625	0.683	160	0.472	0.578	0.614	160	0.553	0.636	0.622	160	0.587	0.639	0.623
320	0.719	Na	0.761	320	0.408	Na	0.508	320	0.550	Na	0.647	320	0.594	Na	0.631
640	0.772	Na	0.781	640	0.456	Na	0.528	640	0.572	Na	0.614	640	0.607	Na	0.628

Table 6: Overall average accuracy of C7, C7-C4, and C7-D4 for predicting the seven high-level properties of the BBOB functions.

	C7	C7-C4	C7-D4
2	0.627	0.634	Na
3	0.651	0.661	0.648
5	0.621	0.632	0.616
10	0.608	Na	0.628
20	0.611	Na	0.623
40	0.628	Na	0.632
80	0.610	Na	0.618
160	0.587	Na	0.593
320	0.594	Na	0.600
640	0.607	Na	0.614

ranked the features based on their impurity-based feature importance values computed by the random forest for each fold, where we used the `feature_importances_` attribute of scikit-learn. Then, we calculated the average rankings of the features over the 24-folds and all the seven classification tasks for each dimension. Table 7 shows only the results of top 10 features. Tables S.3–S.6 show the results of all features for all dimensions.

As seen from Table 7(a), the seven `d_ela_meta` features are ranked as more important than the `d_ela_level` features. For this reason, one may think that the `d_ela_level` features can be removed from C7-D2. However, we observed that removing the `d_ela_level` features from C7-D2 degrades its performance. As shown in Table 7(b), the `d_cm_angle` features are more important than the other cell mapping features. In contrast to C7-D2, all the cell mapping features always rank low. For example, the average ranking of `d_cm_angle.y_ratio_best2worst.sd` is 43.2. However, as demonstrated in Section 6.2.2, the cell mapping features computed by the proposed framework are beneficial for predicting the high-level properties of the BBOB functions. This result indicates the difficulty of feature selection in the ELA approach.

Table 7: Average rankings of the `d_ela_meta` (dem), `d_ela_level` (del), `d_cm_angle` (dca), `d_cm_conv` (dcc), `d_cm_grad` (dcg), and `d_gcm` (dg) features in C7-D2 and C7-D4.

(a) C7-D2		(b) C7-D4	
Feature	Rank	Feature	Rank
<code>dem.lin_simple.coef.max</code>	10.4	<code>dca.y_ratio_best2worst.sd</code>	43.2
<code>dem.lin_simple.intercept</code>	14.0	<code>dca.angle.mean</code>	44.7
<code>dem.lin_simple.coef.min</code>	22.7	<code>dcc.costs_runtime</code>	47.1
<code>dem.quad_simple.adj_r2</code>	22.8	<code>dcg.mean</code>	50.5
<code>dem.quad_w_interact.adj_r2</code>	23.2	<code>dg.near.costs_runtime</code>	50.8
<code>dem.lin_simple.adj_r2</code>	23.9	<code>dca.angle.sd</code>	51.1
<code>dem.lin_w_interact.adj_r2</code>	25.5	<code>dca.dist_ctr2worst.mean</code>	51.4
<code>del.mmce_qda_25</code>	29.7	<code>dca.dist_ctr2best.mean</code>	52.2
<code>del.mmce_lda_50</code>	29.7	<code>dca.y_ratio_best2worst.mean</code>	52.6
<code>del.mmce_mda_50</code>	30.1	<code>dca.dist_ctr2best.sd</code>	52.9

6.2.4 Analysis of m in the proposed framework. The reduced dimension m can be viewed as a control parameter in the proposed framework. Although we set m to 2 in this section, we here investigate the influence of m on the performance of the ELA approach.

Table 8 shows results of C7-D2 and C7-D4 with different m . Tables S.7 and S.8 show detailed results. Since the cell mapping features can be computed for $2 \leq n \leq 5$, we set m to 2, 3, and 5 for C7-D4. Table 8(a) and (b) indicate that a suitable m depends on n and a feature set. Roughly speaking, for C7-D2, $m = 2$ is suitable for $n \leq 320$, but $m = 10$ is the best setting for $n = 640$. Based on this observation, we suggest the use of $m = 2$ for C7-D2, but it may be better to set m to a large value (e.g., $m \in \{5, 10\}$) for $n \geq 640$. For C7-D4, it is difficult to give a general conclusion, but any $m \in \{2, 3, 5\}$ can be a good first choice.

6.3 Similarity of feature values

We analyze the similarity between features and their dimensionality reduction versions. Figure 2 shows values of the `ela_meta.lin_simple.coef.max` feature and its dimensionality reduction version

Table 8: Overall average accuracy of C7-D2 and C7-D4 with different m for $n \in \{5, 10, 20, 40, 80, 160, 320, 640\}$.

	(a) C7-D2					(b) C7-D4		
	1	2	3	5	10	2	3	5
5	0.640	0.635	0.639	Na	Na	0.616	0.623	Na
10	0.654	0.670	0.665	0.643	Na	0.628	0.623	0.621
20	0.655	0.653	0.662	0.652	0.644	0.623	0.618	0.619
40	0.656	0.657	0.649	0.652	0.648	0.632	0.633	0.635
80	0.639	0.649	0.646	0.635	0.636	0.618	0.630	0.627
160	0.617	0.623	0.620	0.626	0.615	0.593	0.596	0.604
320	0.621	0.631	0.629	0.628	0.624	0.600	0.605	0.602
640	0.626	0.628	0.620	0.638	0.642	0.614	0.613	0.611

($m = 2$) on 15 instances of f_1, f_6, f_{10}, f_{15} , and f_{20} with $n = 160$. We selected them from the five function groups, respectively. We also selected `ela_meta.lin_simple.coef.max` based on the results in Section 6.2.3. Figures S.5–S.130 show values of the other features in C7-D2 and C7-D4. As seen from the scale of the y-axis in Figures 2(a) and (b), values of the original feature and its dimensionality reduction version are totally different. The cause of this observation may be the PCA transformation. An analysis of the proposed framework with nonlinear transformation techniques (e.g., t-SNE [46]) is an avenue for future work. However, the relative rankings of the feature values on f_1, f_6, f_{10}, f_{15} , and f_{20} are similar in Figures 2(a) and (b). For example, the two features take the smallest and largest values on f_1 and f_{10} , respectively.

Figure 3 shows the Kendall rank correlation coefficient τ values of the 8 `ela_meta` and `d_ela_meta` features on the 24 BBOB functions with $n = 160$. Since 3 out of the 11 `ela_meta` and `d_ela_meta` features include non-unique values, we could not calculate their τ values. Let $\mathbf{a} = (a_1, \dots, a_{24})^\top$ and $\mathbf{b} = (b_1, \dots, b_{24})^\top$ be the values of the original feature and its dimensionality reduction version on the 24 BBOB functions respectively, where $a_i \in \mathbf{a}$ and $b_i \in \mathbf{b}$ are the average over 15 instances of f_i ($i \in \{1, \dots, 24\}$). The τ value quantifies the similarity of the rankings of \mathbf{a} and \mathbf{b} . Here, τ takes a value in the range $[-1, 1]$. If the rankings of \mathbf{a} and \mathbf{b} are perfectly consistent, $\tau = 1$. If they are perfectly inconsistent, $\tau = -1$. If they are perfectly independent, $\tau = 0$.

As shown in Figure 3, `ela_meta.lin_simple.coef.max` is strongly consistent with `d_ela_meta.lin_simple.coef.max` ($\tau = 0.96$). We can see high τ values for the following three features: `lin_simple.adj_r2`, `lin_simple.intercept`, and `lin_simple.coef.min`. These results indicate that the relative rankings of values of some features and their dimensionality reduction versions can possibly be similar even if their absolute values are different. We believe that a feature computed by the proposed framework can substitute for its original version when their relative rankings are similar.

Note that this is not always the case. Since τ is close to zero for `lin_simple.coef.max_by_min`, `quad_simple.cond`, and `costs_runtime` (see (e), (g), and (h) in Figure 3), their original and dimensionality reduction versions are almost independent. Figures S.131–S.135 show results of the other features. The results of `d_ela_level` and `d_gcm` are relatively similar to Figure 3. In contrast, we observed that τ is close to zero for most features in the `d_cm_angle`, `d_cm_grad`, and `d_cm_conv` classes. It would be better to consider that the dimensionality reduction versions of these features are not related to their original versions.

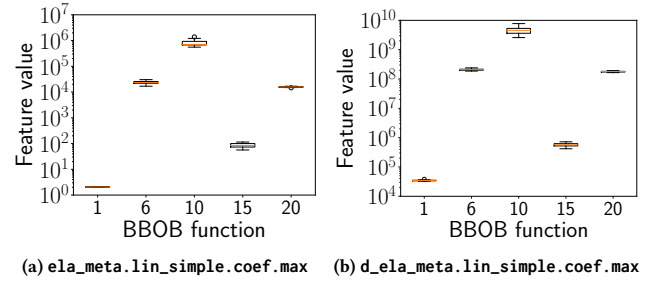


Figure 2: Boxplots of values of `ela_meta.lin_simple.coef.max` and its dimensionality reduction version on 15 instances of f_1, f_6, f_{10}, f_{15} , and f_{20} with $n = 160$.

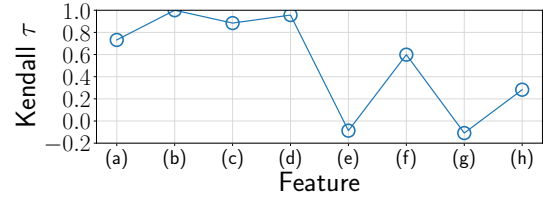


Figure 3: Kendall τ values of `ela_meta` and `d_ela_meta` for $n = 160$, where (a) `lin_simple.adj_r2`, (b) `lin_simple.intercept`, (c) `lin_simple.coef.min`, (d) `lin_simple.coef.max`, (e) `lin_simple.coef.max_by_min`, (f) `quad_simple.adj_r2`, (g) `quad_simple.cond`, and (h) `costs_runtime`.

7 CONCLUSION

First, we pointed out the computational cost issue in the ELA features for large dimensions. Our results revealed that the two important feature classes (`ela_level` and `ela_meta`) cannot be applied to large-scale optimization due to their high computational cost. To address this issue, we proposed the dimensionality reduction framework that computes features in a reduced low-dimensional space. Our results show that the proposed framework can drastically reduce the computation time of `ela_level` and `ela_meta`. Our results also show the effectiveness of features (including the four cell mapping features) computed by the proposed framework on the BBOB functions with up to 640 dimensions. In addition, we found that the relative rankings of values of some (not all) features and their dimensionality reduction versions are similar.

We focused on extending the existing features for large dimensions, but it is promising to design a new computationally cheap feature. An extension of landscape-aware algorithm selection methods for large-scale optimization is an avenue for future work. It is not obvious if the classification accuracy shown in this paper is good enough for practical purposes. There is room for discussion about the benchmarking methodology of the ELA approach.

ACKNOWLEDGMENTS

This work was supported by Leading Initiative for Excellent Young Researchers, MEXT, Japan.

REFERENCES

- [1] Brian Beachkofski and Ramana Grandhi. 2002. Improved Distributed Hypercube Sampling. In *AIAA/ASME/ASCE/AHS/ASC Structures, Structural Dynamics, and Materials Conference*. 1274. <https://doi.org/10.2514/6.2002-1274>
- [2] Nacim Belkhir, Johann Dréo, Pierre Savéant, and Marc Schoenauer. 2016. Feature Based Algorithm Configuration: A Case Study with Differential Evolution. In *Parallel Problem Solving from Nature - PPSN XIV - 14th International Conference, Edinburgh, UK, September 17-21, 2016, Proceedings (Lecture Notes in Computer Science, Vol. 9921)*, Julia Handl, Emma Hart, Peter R. Lewis, Manuel López-Ibáñez, Gabriela Ochoa, and Ben Paechter (Eds.). Springer, 156–166. https://doi.org/10.1007/978-3-319-45823-6_15
- [3] Nacim Belkhir, Johann Dréo, Pierre Savéant, and Marc Schoenauer. 2016. Surrogate Assisted Feature Computation for Continuous Problems. In *Learning and Intelligent Optimization - 10th International Conference, LION 10, Ischia, Italy, May 29 - June 1, 2016, Revised Selected Papers (Lecture Notes in Computer Science, Vol. 10079)*, Paola Festa, Meinolf Sellmann, and Joaquin Vanschoren (Eds.). Springer, 17–31. https://doi.org/10.1007/978-3-319-50349-3_2
- [4] Nacim Belkhir, Johann Dréo, Pierre Savéant, and Marc Schoenauer. 2017. Per instance algorithm configuration of CMA-ES with limited budget. In *Proceedings of the Genetic and Evolutionary Computation Conference, GECCO 2017, Berlin, Germany, July 15-19, 2017*, Peter A. N. Bosman (Ed.). ACM, 681–688. <https://doi.org/10.1145/3071178.3071343>
- [5] Bernd Bischl, Olaf Mersmann, Heike Trautmann, and Mike Preuß. 2012. Algorithm selection based on exploratory landscape analysis and cost-sensitive learning. In *Genetic and Evolutionary Computation Conference, GECCO '12, Philadelphia, PA, USA, July 7-11, 2012*, Terence Soule and Jason H. Moore (Eds.). ACM, 313–320. <https://doi.org/10.1145/2330163.2330209>
- [6] Leo Breiman. 2001. Random Forests. *Machine Learning* 45, 1 (2001), 5–32. <https://doi.org/10.1023/A:1010933404324>
- [7] Bilel Derbel, Arnaud Liefiooghe, Sébastien Vétel, Hernán E. Aguirre, and Kiyoshi Tanaka. 2019. New features for continuous exploratory landscape analysis based on the SOO tree. In *Proceedings of the 15th ACM/SIGEVO Conference on Foundations of Genetic Algorithms, FOGA 2019, Potsdam, Germany, August 27-29, 2019*, Tobias Friedrich, Carola Doerr, and Dirk V. Arnold (Eds.). ACM, 72–86. <https://doi.org/10.1145/3299904.3340308>
- [8] Tome Eftimov, Gorjan Popovski, Quentin Renau, Peter Korošec, and Carola Doerr. 2020. Linear Matrix Factorization Embeddings for Single-objective Optimization Landscapes. In *2020 IEEE Symposium Series on Computational Intelligence, SSCI 2020, Canberra, Australia, December 1-4, 2020*. IEEE, 775–782. <https://doi.org/10.1109/SSCI47803.2020.9308180>
- [9] Sim Kuan Goh, Kay Chen Tan, Abdullah Al Mamun, and Hussein A. Abbass. 2015. Evolutionary Big Optimization (BigOpt) of Signals. In *IEEE Congress on Evolutionary Computation, CEC 2015, Sendai, Japan, May 25-28, 2015*. IEEE, 3332–3339. <https://doi.org/10.1109/CEC.2015.7257307>
- [10] Nikolaus Hansen, Anne Auger, Raymond Ros, Olaf Mersmann, Tea Tušar, and Dimo Brockhoff. 2021. COCO: a platform for comparing continuous optimizers in a black-box setting. *Optimization Methods and Software* 36, 1 (2021), 114–144. <https://doi.org/10.1080/10556788.2020.1808977>
- [11] N. Hansen, S. Finck, R. Ros, and A. Auger. 2009. *Real-Parameter Black-Box Optimization Benchmarking 2009: Noiseless Functions Definitions*. Technical Report RR-6829. INRIA. <https://hal.inria.fr/inria-00362633>
- [12] Wen-bing Huang, Deli Zhao, Fuchun Sun, Huaping Liu, and Edward Y. Chang. 2015. Scalable Gaussian Process Regression Using Deep Neural Networks. In *Proceedings of the Twenty-Fourth International Joint Conference on Artificial Intelligence, IJCAI 2015, Buenos Aires, Argentina, July 25-31, 2015*, Qiang Yang and Michael J. Wooldridge (Eds.). AAAI Press, 3576–3582. <http://ijcai.org/Abstract/15/503>
- [13] Anja Jankovic and Carola Doerr. 2020. Landscape-aware fixed-budget performance regression and algorithm selection for modular CMA-ES variants. In *GECCO '20: Genetic and Evolutionary Computation Conference, Cancún Mexico, July 8-12, 2020*, Carlos Artemio Coello Coello (Ed.). ACM, 841–849. <https://doi.org/10.1145/3377930.3390183>
- [14] Anja Jankovic, Tome Eftimov, and Carola Doerr. 2021. Towards Feature-Based Performance Regression Using Trajectory Data. In *Applications of Evolutionary Computation - 24th International Conference, EvoApplications 2021, Held as Part of EvoStar 2021, Virtual Event, April 7-9, 2021, Proceedings (Lecture Notes in Computer Science, Vol. 12694)*, Pedro A. Castillo and Juan Luis Jiménez Laredo (Eds.). Springer, 601–617. https://doi.org/10.1007/978-3-030-72699-7_38
- [15] Terry Jones and Stephanie Forrest. 1995. Fitness Distance Correlation as a Measure of Problem Difficulty for Genetic Algorithms. In *Proceedings of the 6th International Conference on Genetic Algorithms, Pittsburgh, PA, USA, July 15-19, 1995*, Larry J. Eshelman (Ed.). Morgan Kaufmann, 184–192.
- [16] Pascal Kerschke, Mike Preuss, Carlos Hernández, Oliver Schütze, Jian-Qiao Sun, Christian Grimme, Günter Rudolph, Bernd Bischl, and Heike Trautmann. 2014. Cell Mapping Techniques for Exploratory Landscape Analysis. In *EVOLVE - A Bridge between Probability, Set Oriented Numerics, and Evolutionary Computation V*, Alexandru-Adrian Tantar, Emilia Tantar, Jian-Qiao Sun, Wei Zhang, Qian Ding, Oliver Schütze, Michael Emmerich, Pierrick Legrand, Pierre Del Moral, and Carlos A. Coello Coello (Eds.), 115–131.
- [17] Pascal Kerschke, Mike Preuss, Simon Wessing, and Heike Trautmann. 2015. Detecting Funnel Structures by Means of Exploratory Landscape Analysis. In *Proceedings of the Genetic and Evolutionary Computation Conference, GECCO 2015, Madrid, Spain, July 11-15, 2015*, Sara Silva and Anna Isabel Esparcia-Alcázar (Eds.). ACM, 265–272. <https://doi.org/10.1145/2739480.2754642>
- [18] Pascal Kerschke, Mike Preuss, Simon Wessing, and Heike Trautmann. 2016. Low-Budget Exploratory Landscape Analysis on Multiple Peaks Models. In *Proceedings of the 2016 on Genetic and Evolutionary Computation Conference, Denver, CO, USA, July 20 - 24, 2016*, Tobias Friedrich, Frank Neumann, and Andrew M. Sutton (Eds.). ACM, 229–236. <https://doi.org/10.1145/2908812.2908845>
- [19] Pascal Kerschke and Heike Trautmann. 2019. Automated Algorithm Selection on Continuous Black-Box Problems by Combining Exploratory Landscape Analysis and Machine Learning. *Evolutionary Computation* 27, 1 (2019), 99–127. https://doi.org/10.1162/evco_a_00236
- [20] Pascal Kerschke and Heike Trautmann. 2019. Comprehensive Feature-Based Landscape Analysis of Continuous and Constrained Optimization Problems Using the R-package flacco. In *Applications in Statistical Computing - From Music Data Analysis to Industrial Quality Improvement*, Nadja Bauer, Katja Ickstadt, Karsten Lübke, Gero Szepannek, Heike Trautmann, and Maurizio Vichi (Eds.). Springer, 93–123. https://doi.org/10.1007/978-3-030-25147-5_7
- [21] Bo Liu, Qingfu Zhang, and Georges G. E. Gielen. 2014. A Gaussian Process Surrogate Model Assisted Evolutionary Algorithm for Medium Scale Expensive Optimization Problems. *IEEE Transaction Evolutionary Computation* 18, 2 (2014), 180–192. <https://doi.org/10.1109/TEVC.2013.2248012>
- [22] Monte Lunacek and L. Darrell Whitley. 2006. The dispersion metric and the CMA evolution strategy. In *Genetic and Evolutionary Computation Conference, GECCO 2006, Proceedings, Seattle, Washington, USA, July 8-12, 2006*, Mike Cattolico (Ed.). ACM, 477–484. <https://doi.org/10.1145/1143997.1144085>
- [23] Monte Lunacek, L. Darrell Whitley, and Andrew M. Sutton. 2008. The Impact of Global Structure on Search. In *Parallel Problem Solving from Nature - PPSN X, 10th International Conference Dortmund, Germany, September 13-17, 2008, Proceedings (Lecture Notes in Computer Science, Vol. 5199)*, Günter Rudolph, Thomas Jansen, Simon M. Lucas, Carlo Poloni, and Nicola Beume (Eds.). Springer, 498–507. https://doi.org/10.1007/978-3-540-87700-4_50
- [24] Katherine Malan and Andries Petrus Engelbrecht. 2013. A survey of techniques for characterising fitness landscapes and some possible ways forward. *Information Sciences* 241 (2013), 148–163. <https://doi.org/10.1016/j.ins.2013.04.015>
- [25] Olaf Mersmann, Bernd Bischl, Heike Trautmann, Mike Preuss, Claus Weihs, and Günter Rudolph. 2011. Exploratory landscape analysis. In *13th Annual Genetic and Evolutionary Computation Conference, GECCO 2011, Proceedings, Dublin, Ireland, July 12-16, 2011*, Natalio Krasnogor and Pier Luca Lanzi (Eds.). ACM, 829–836. <https://doi.org/10.1145/2001576.2001690>
- [26] Olaf Mersmann, Mike Preuss, and Heike Trautmann. 2010. Benchmarking Evolutionary Algorithms: Towards Exploratory Landscape Analysis. In *Parallel Problem Solving from Nature - PPSN XI, 11th International Conference, Kraków, Poland, September 11-15, 2010, Proceedings, Part I (Lecture Notes in Computer Science, Vol. 6238)*, Robert Schaefer, Carlos Cotta, Joanna Kolodziej, and Günter Rudolph (Eds.). Springer, 73–82. https://doi.org/10.1007/978-3-642-15844-5_8
- [27] Olaf Mersmann, Mike Preuss, Heike Trautmann, Bernd Bischl, and Claus Weihs. 2015. Analyzing the BBOB Results by Means of Benchmarking Concepts. *Evolutionary Computation* 23, 1 (2015), 161–185. https://doi.org/10.1162/EVCO_a_00134
- [28] Rachael Morgan and Marcus Gallagher. 2012. Length Scale for Characterising Continuous Optimization Problems. In *Parallel Problem Solving from Nature - PPSN XII - 12th International Conference, Taormina, Italy, September 1-5, 2012, Proceedings, Part I (Lecture Notes in Computer Science, Vol. 7491)*, Carlos A. Coello Coello, Vincenzo Cutello, Kalyanmoy Deb, Stephanie Forrest, Giuseppe Nicosia, and Mario Pavone (Eds.). Springer, 407–416. https://doi.org/10.1007/978-3-642-32937-1_41
- [29] Rachael Morgan and Marcus Gallagher. 2014. Sampling Techniques and Distance Metrics in High Dimensional Continuous Landscape Analysis: Limitations and Improvements. *IEEE Transaction Evolutionary Computation* 18, 3 (2014), 456–461. <https://doi.org/10.1109/TEVC.2013.2281521>
- [30] Christian L. Müller and Ivo F. Sbalzarini. 2011. Global Characterization of the CEC 2005 Fitness Landscapes Using Fitness-Distance Analysis. In *Applications of Evolutionary Computation - EvoApplications 2011: EvoCOMPLEX, EvoGAMES, EvoIASP, EvoINTELLIGENCE, EvoNUM, and EvoSTOC, Torino, Italy, April 27-29, 2011, Proceedings, Part I (Lecture Notes in Computer Science, Vol. 6624)*, Cecilia Di Chio, Stefano Cagnoni, Carlos Cotta, Marc Ebner, Anikó Ekárt, Anna Esparcia-Alcázar, Juan Julián Merelo Guervós, Ferrante Neri, Mike Preuss, Hendrik Richter, Julian Togelius, and Georgios N. Yannakakis (Eds.). Springer, 294–303. https://doi.org/10.1007/978-3-642-20525-5_30
- [31] Nils Müller and Tobias Glasmachers. 2018. Challenges in High-Dimensional Reinforcement Learning with Evolution Strategies. In *Parallel Problem Solving from Nature - PPSN XV - 15th International Conference, Coimbra, Portugal, September 8-12, 2018, Proceedings, Part II (Lecture Notes in Computer Science, Vol. 11102)*, Anne

- Auger, Carlos M. Fonseca, Nuno Lourenço, Penousal Machado, Luís Paquete, and L. Darrell Whitley (Eds.). Springer, 411–423. https://doi.org/10.1007/978-3-319-99259-4_33
- [32] Mario A. Muñoz, Michael Kirley, and Saman K. Halgamuge. 2012. A Meta-learning Prediction Model of Algorithm Performance for Continuous Optimization Problems. In *Parallel Problem Solving from Nature - PPSN XII - 12th International Conference, Taormina, Italy, September 1-5, 2012, Proceedings, Part 1 (Lecture Notes in Computer Science, Vol. 7491)*, Carlos A. Coello Coello, Vincenzo Cutello, Kalyanmoy Deb, Stephanie Forrest, Giuseppe Nicosia, and Mario Pavone (Eds.). Springer, 226–235. https://doi.org/10.1007/978-3-642-32937-1_23
- [33] Mario A. Muñoz, Michael Kirley, and Saman K. Halgamuge. 2015. Exploratory Landscape Analysis of Continuous Space Optimization Problems Using Information Content. *IEEE Transaction Evolutionary Computation* 19, 1 (2015), 74–87. <https://doi.org/10.1109/TEVC.2014.2302006>
- [34] Mario A. Muñoz and Kate Smith-Miles. 2015. Effects of function translation and dimensionality reduction on landscape analysis. In *IEEE Congress on Evolutionary Computation, CEC 2015, Sendai, Japan, May 25-28, 2015*. IEEE, 1336–1342. <https://doi.org/10.1109/CEC.2015.7257043>
- [35] Fabian Pedregosa, Gaël Varoquaux, Alexandre Gramfort, Vincent Michel, Bertrand Thirion, Olivier Grisel, Mathieu Blondel, Peter Prettenhofer, Ron Weiss, Vincent Dubourg, Jake VanderPlas, Alexandre Passos, David Cournapeau, Matthieu Brucher, Matthieu Perrot, and Edouard Duchesnay. 2011. Scikit-learn: Machine Learning in Python. *Journal of Machine Learning Research* 12 (2011), 2825–2830. <http://dl.acm.org/citation.cfm?id=2078195>
- [36] Erik Pitzer and Michael Affenzeller. 2012. A Comprehensive Survey on Fitness Landscape Analysis. In *Recent Advances in Intelligent Engineering Systems*, János C. Fodor, Ryszard Klempous, and Carmen Paz Suárez Araujo (Eds.). Studies in Computational Intelligence, Vol. 378. Springer, 161–191. https://doi.org/10.1007/978-3-642-23229-9_8
- [37] Mike Preuss. 2012. Improved Topological Niching for Real-Valued Global Optimization. In *Applications of Evolutionary Computation - EvoApplications 2012: EvoCOMNET, EvoCOMPLEX, EvoFIN, EvoGAMES, EvoHOT, EvoASP, EvoNUM, EvoPAR, EvoRISK, EvoSTIM, and EvoSTOC, Málaga, Spain, April 11-13, 2012, Proceedings (Lecture Notes in Computer Science, Vol. 7248)*, Cecilia Di Chio, Alexandros Agapitos, Stefano Cagnoni, Carlos Cotta, Francisco Fernández de Vega, Gianni A. Di Caro, Rolf Drechsler, Anikó Ekárt, Anna Isabel Esparcia-Alcázar, Muddassar Farooq, William B. Langdon, Juan Julián Merelo Guervós, Mike Preuss, Hendrik Richter, Sara Silva, Anabela Simões, Giovanni Squillero, Ernesto Tarantino, Andrea Tettamanzi, Julian Togelius, Neil Urquhart, Sima Uyar, and Georgios N. Yannakakis (Eds.). Springer, 386–395. https://doi.org/10.1007/978-3-642-29178-4_39
- [38] Elena Raponi, Hao Wang, Mariusz Bujny, Simonetta Boria, and Carola Doerr. 2020. High Dimensional Bayesian Optimization Assisted by Principal Component Analysis. In *Parallel Problem Solving from Nature - PPSN XVI - 16th International Conference, PPSN 2020, Leiden, The Netherlands, September 5-9, 2020, Proceedings, Part 1 (Lecture Notes in Computer Science, Vol. 12269)*, Thomas Bäck, Mike Preuss, André H. Deutz, Hao Wang, Carola Doerr, Michael T. M. Emmerich, and Heike Trautmann (Eds.). Springer, 169–183. https://doi.org/10.1007/978-3-030-58112-1_12
- [39] Quentin Renau, Carola Doerr, Johann Dréo, and Benjamin Doerr. 2020. Exploratory Landscape Analysis is Strongly Sensitive to the Sampling Strategy. In *Parallel Problem Solving from Nature - PPSN XVI - 16th International Conference, PPSN 2020, Leiden, The Netherlands, September 5-9, 2020, Proceedings, Part II (Lecture Notes in Computer Science, Vol. 12270)*, Thomas Bäck, Mike Preuss, André H. Deutz, Hao Wang, Carola Doerr, Michael T. M. Emmerich, and Heike Trautmann (Eds.). Springer, 139–153. https://doi.org/10.1007/978-3-030-58115-2_10
- [40] Bobak Shahriari, Kevin Swersky, Ziyu Wang, Ryan P. Adams, and Nando de Freitas. 2016. Taking the Human Out of the Loop: A Review of Bayesian Optimization. *Proc. IEEE* 104, 1 (2016), 148–175. <https://doi.org/10.1109/JPROC.2015.2494218>
- [41] Shinichi Shirakawa and Tomoharu Nagao. 2016. Bag of local landscape features for fitness landscape analysis. *Soft Computing* 20, 10 (2016), 3787–3802. <https://doi.org/10.1007/s00500-016-2091-4>
- [42] Jonathon Shlens. 2014. A Tutorial on Principal Component Analysis. *CoRR* abs/1404.1100 (2014). arXiv:1404.1100 <http://arxiv.org/abs/1404.1100>
- [43] Tom Smith, Phil Husbands, Paul J. Layzell, and Michael O’Shea. 2002. Fitness Landscapes and Evolvability. *Evolutionary Computation* 10, 1 (2002), 1–34. <https://doi.org/10.1162/106365602317301754>
- [44] Mohammad-H. Tayarani-N. and Adam Prügel-Bennett. 2016. An Analysis of the Fitness Landscape of Travelling Salesman Problem. *Evolutionary Computation* 24, 2 (2016), 347–384. https://doi.org/10.1162/EVCO_a_00154
- [45] Sibghat Ullah, Duc Anh Nguyen, Hao Wang, Stefan Menzel, Bernhard Sendhoff, and Thomas Bäck. 2020. Exploring Dimensionality Reduction Techniques for Efficient Surrogate-Assisted optimization. In *2020 IEEE Symposium Series on Computational Intelligence, SSCI 2020, Canberra, Australia, December 1-4, 2020*. IEEE, 2965–2974. <https://doi.org/10.1109/SSCI47803.2020.9308465>
- [46] Laurens van der Maaten and Geoffrey Hinton. 2008. Visualizing Data using t-SNE. *Journal of Machine Learning Research* 9, 86 (2008), 2579–2605.
- [47] Laurens van der Maaten, Eric Postma, and Jaap van den Herik. 2008. *Dimensionality Reduction: A Comparative Review*. Technical Report. Tilburg University.
- [48] Konstantinos Varelas, Ouassim Ait ElHara, Dimo Brockhoff, Nikolaus Hansen, Duc Manh Nguyen, Tea Tušar, and Anne Auger. 2020. Benchmarking large-scale continuous optimizers: The bbob-largescale testbed, a COCO software guide and beyond. *Applied Soft Computing* 97, Part (2020), 106737. <https://doi.org/10.1016/j.asoc.2020.106737>
- [49] Nadarajen Veerapen and Gabriela Ochoa. 2018. Visualising the global structure of search landscapes: genetic improvement as a case study. *Genetic Programming and Evolvable Machines* 19, 3 (2018), 317–349. <https://doi.org/10.1007/s10710-018-9328-1>
- [50] Urban Škvorc, Tome Eftimov, and Peter Korošec. 2020. Understanding the problem space in single-objective numerical optimization using exploratory landscape analysis. *Applied Soft Computing* 90 (2020), 106138. <https://doi.org/10.1016/j.asoc.2020.106138>
- [51] Ziyu Wang, Frank Hutter, Masrouf Zoghi, David Matheson, and Nando de Freitas. 2016. Bayesian Optimization in a Billion Dimensions via Random Embeddings. *Journal of Artificial Intelligence Research* 55 (2016), 361–387. <https://doi.org/10.1613/jair.4806>